

Enhancement and Suppression of Transmission in 3-D Nanoslits Arrays with 1- and 2-D Periodicities

M.A. Vincenti*, D. de Ceglia

AEGIS Technologies Group, 410 Jan Davis Dr., Huntsville, AL 35806

M. Scalora

Charles M. Bowden Research Center AMSRD-AMR-WS-ST, RDECOM, Redstone Arsenal,
Alabama 35898-5000, USA

R. Marani, V. Marrocco, M. Grande, G. Morea, and A. D'Orazio

Dipartimento di Elettrotecnica ed Elettronica, Politecnico di Bari, Via Orabona 4, 70125 Bari, Italy

ABSTRACT

We investigate the transmission properties of arrays of three-dimensional (3-D) gold patches having one- and two-dimensional (1- and 2-D) periodicities, and describe the interaction of cavity and surface plasmon modes. We vary the main geometrical parameters to assess similarities and emphasize differences between 1-D and 2-D periodic patterns. We analyze the spectral response as a function of incident angle and polarization to corroborate our findings. We will also consider form and air filling factors of the grating to assess our ability to control the transmission spectrum. In particular, we observe strong inhibition of the transmission when the impinging wave-vector parallel to the surface of the metal matches the surface plasmon wave-vector of the unperturbed air-gold interface when added to the grating lattice wave-vector. This phenomenon favors the opening of a plasmonic band gap, featuring the suppression of transmission and simultaneous coupling to back-radiation (reflections) of the unperturbed surface plasmon. High-Q, resonating modes occur at the edges of the forbidden band, boosting the energy transfer across the grating thus providing enhanced transmission and broadside directivity at the exit side of the grating.

Keywords: Surface Plasmon, enhanced transmission, plasmonic band gap, resonant cavity modes

1. INTRODUCTION

During the last decade many efforts have been devoted to the study and the optimization of metal gratings to find way to enhance transmittance in environments dominated and limited by absorption and diffraction. Transmission and reflection properties of metal films with arrays of sub-wavelength apertures have been under intense scrutiny ever since Ebbesen et al.¹ demonstrated experimentally that light coupling to surface plasmons (SPs) gives rise to unexpectedly high transmission. Following Ebbesen initial report, the same peculiar mechanism has been observed in different topologies, such as sub-wavelength slits, where the excitation of guided, resonant modes allows coupling of light also below the theoretical diffraction limit^{2,3}. The transport of light with great accuracy to a desired location is an important issue across a wide spectrum of applications that range from commercial to military platforms. Nano-patterned metal layers can be designed *ad hoc* for applications like sensing⁴, beam steering⁵ and photovoltaics⁶, to mention a few. Indeed 1- and 2-D periodic structures are good candidates to achieve control of light localization and deflection and to manage the spectral response. Although numerous theoretical and experimental studies report on the optical response of metal gratings patterned with sub-wavelength slits⁷⁻⁹, the effects of different periodicities in the same structure and the similarities of 1-D and 2-D periodic arrays have not been fully understood. We presently undertake an effort to compare spectral and field localization properties of 3-D arrays composed of gold patches having 1-D and 2-D periodicity and show how the coupling phenomena between Fabry-Pérot (FP) resonant modes and SPs propagating along the grating surface are influenced by the patches form factor and field excitation conditions.

*mvincenti@aegistg.com; phone 1 256 955-6278

2. 1- AND 2-D PERIODICITIES IN NANOSLITS ARRAYS

In this paper we introduce the comparison between nanoslits arrays showing 1-D (Fig.1(a)) and 2-D (Fig.1(b)) periodicities. We proceed by first considering a 2-D array made of square patches having the same thickness and aperture size of the equivalent 1-D structure, where a is the aperture size, w is the thickness of the metal layer or patch, p is the periodicity of the 1-D grating (Fig.1(a)). At the same time, with reference to Fig.1(b), a is the gap between two adjacent patches, whereas p_1 and p_2 are respectively the periodicities of the 2-D array. For simplicity in what follows we will assume $a = 150 \text{ nm}$, $w = 180 \text{ nm}$, while p , p_1 and p_2 will be varied so that the properties of 1-D and 2-D gratings may be assessed. We stress that this choice of parameters is not unique and other combinations of a and w may be used to demonstrate the same properties shown below. The permittivity of gold¹⁰ was fitted using a Drude model (for free electrons) and two Lorentz-like oscillators to account for interband transitions at near IR and visible wavelengths. All simulations were performed using a commercial three-dimensional FEM analysis¹¹.

The excitation of surface waves and the access to the extraordinary transmission regime in these metal structures is strongly influenced by field polarization. It is well known that surface plasmons may be excited by TM-polarized incident waves (see inset in Fig.1(a)). In order to excite these surface waves in both configurations we consider the incident field polarized as depicted in the insets of Fig.1(a) and (b), with the Poynting vector always orthogonal to the metal surface. The inset of Fig.1(b) also shows the orientation of the electric field by means of the rotation angle θ ; this angle will help us to assess the sensitivity of the transmission features as a function of this angle, so that the electric field components parallel to the periodicities have different intensities.

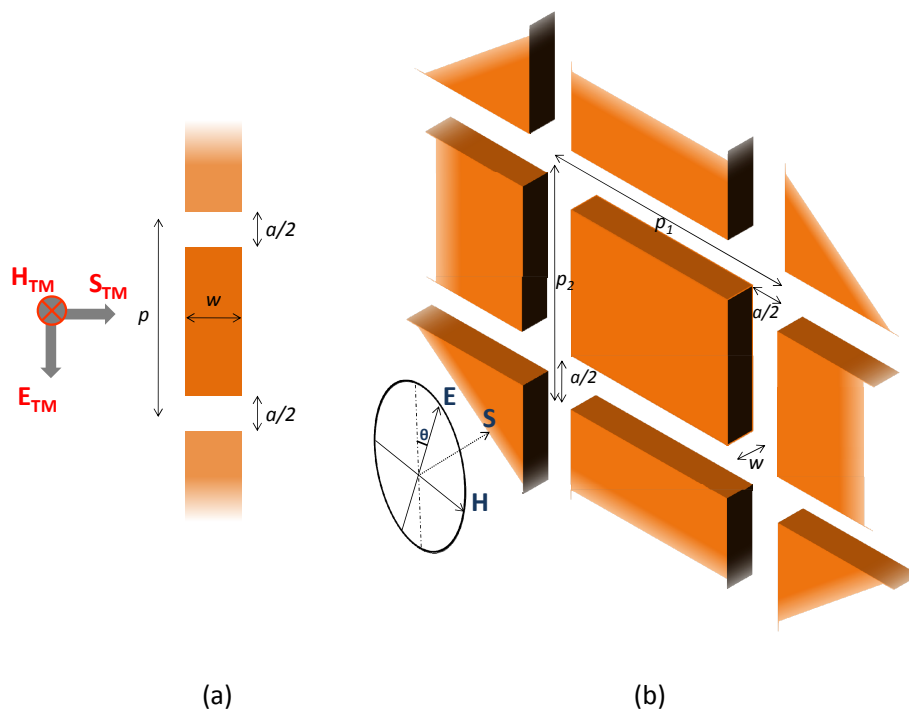


Fig.1. Sketch of (a) 1-D- periodic structure: a is the aperture size, w is the thickness of the metal layer and p is the periodicity. The arrows on the left define the impinging field polarization; (b) 2-D periodic structure: a is gap between two adjacent patches, w is the thickness of the patch, p_1 and p_2 are the periodicities of the gold patch; Electric and magnetic field orientation are depicted in the inset together with θ . This angle will help us to analyze the sensitivity of the spectrum to the angle of the electric field.

Let us first consider a 1-D periodic array of slits (Fig.1(a)), carved on a gold layer. Fig.2(a) shows the transmission spectrum from 760 nm to 1200 nm for two different array periodicities. The periodicity $p = 800 \text{ nm}$ (blue line) allows the observation of a zero transmission state at $m_1 = 814.5 \text{ nm}$. The periodicity $p = 1000 \text{ nm}$ (red line) creates a zero transmission state at $m_2 = 1010.7 \text{ nm}$. Both these minima open a plasmonic band gap caused by the interaction of FP-like cavity modes and surface waves propagating along the metal surface. The spectral position of the transmission resonances of the slits occurs when $w = \frac{m\lambda_0}{2n_{\text{eff}}}$, where m is an integer, n_{eff} is the effective index of the plasmonic metal-

air-metal waveguide formed by each slit. These transmission peaks are governed by both geometrical parameters a and w . As already pointed out elsewhere^{12,13}, these kinds of resonances are characterized by significant field localization inside the isolated slit. Enhanced transmission occurs without any contributions from surface corrugations or any grating effects. In a single slit, in fact, the transmission process is mostly driven by the TM fundamental mode, whose dispersion is strongly influenced by metal conductivity and slit size. On the other hand a multiple slit geometry structured either in a 1- or 2-D periodic arrangement introduces the pitch as an additional degree of freedom. Adding more slits does not enhance significantly the transmission value itself, which indeed tends to saturate for more than 6 slits^{8,12}. However, this argument does not hold under certain circumstances: if pitch size interferes with Fabry-Pérot-like resonances, the spectral response can be significantly altered, as demonstrated in Ref. 14 for a PEC grating and for metals at microwave or THz frequencies, and as Fig.2(a) shows for our structure. Transmission minima are in fact found at the wavelengths m_1 and m_2 , where a matching condition between pitch size, incident wavelength and the unperturbed surface plasmon polaritons (SPPs) effective wavelength is satisfied. In fact by looking at the dispersion curve of the effective refractive index of a surface plasmon for an air/gold interface (Fig.2(b)) one may conclude that m_1 and m_2 match perfectly array periodicity when normalized to the effective index of the surface plasmon propagating wavelength: for both these points the relation $\lambda_{\text{min}} = p \cdot n_{\text{spp gold/air}}$ is verified. In particular, the formation of a zero-transmission state corresponds to the rising of a standing wave on the air-metal interface that radiates backward, showing a spectral behavior resembling a plasmonic band gap reflector.

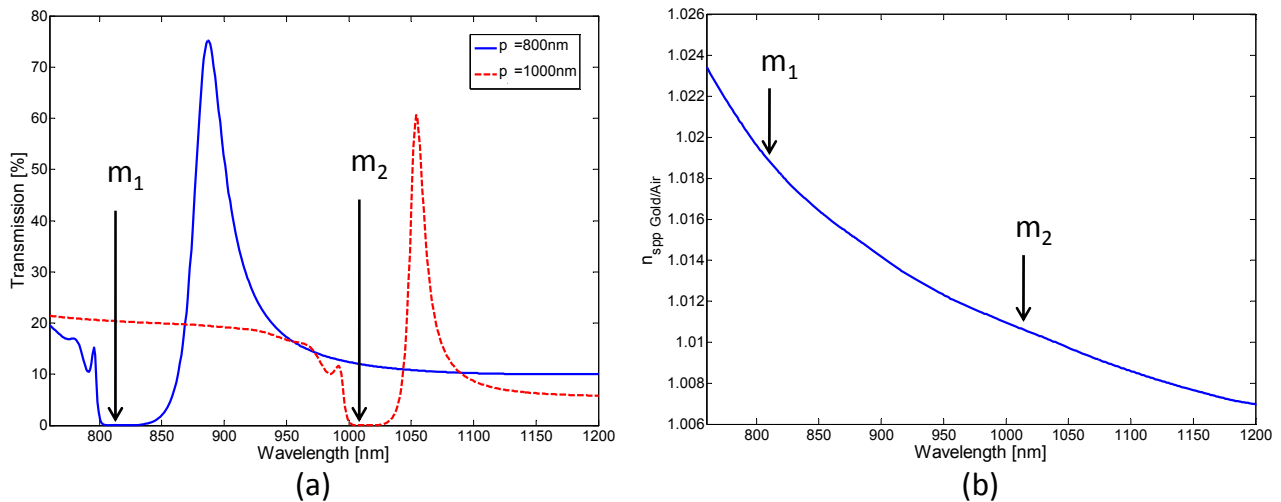


Fig.2. (a) Transmission spectra for 1-D- periodic arrays having $p = 800 \text{ nm}$ (blue line) and $p = 1000 \text{ nm}$ (red line). Two transmission minima (m_1 and m_2) and band gaps are evident in the spectra. (b) Gold/air surface plasmon effective index dispersion: m_1 and m_2 are the wavelengths of the two minima in (a).

Let us now consider more in details the behavior of 2-D periodic structures in order to compare the properties of 1- and 2-D arrays. We begun our study by considering gold square patches having $p_1 = p_2$. This restriction allows us compare a 2-D periodic array with 1-D one. This comparison reveals almost identical spectra, regardless of the periodicity used (see Fig.3(a) and Fig.3(b) where the periodicities are respectively $p = p_1 = p_2 = 800 \text{ nm}$ and $p = p_1 = p_2 = 1000 \text{ nm}$). Black-dashed lines of both Figs.3(a) and 3(b) are obtained for a rotation angle $\theta = 0$, but, as we will clarify later, all the features of the spectrum of the 2-D periodic array remain unaltered by rotating the electric field in the plane parallel to the metal surface. The strong analogies between 1- and 2-D periodic arrays can be explained by observing the polarization of the incident field use to analyze the 2-D structure. In fact, with reference to Fig.1(b), when the rotation

angle θ is equal to zero, the maximum coupling between gold elements is only achieved along the direction of p_2 , whereas the direction of p_1 does not introduce any modification to the matching condition described previously for the 1-D periodic array. This aspect is mainly due to the orientation of the magnetic field, which is actually parallel to the nanoslit array arranged with a lattice constant equal to p_1 . Hence, in this case, SPs can be sustained, playing a key-role in the bandgap formation. On the contrary, as a result of the application of boundary conditions, SPs are negligible for the other polarization component, which lies along p_2 when $\theta = 0$ ¹⁵.

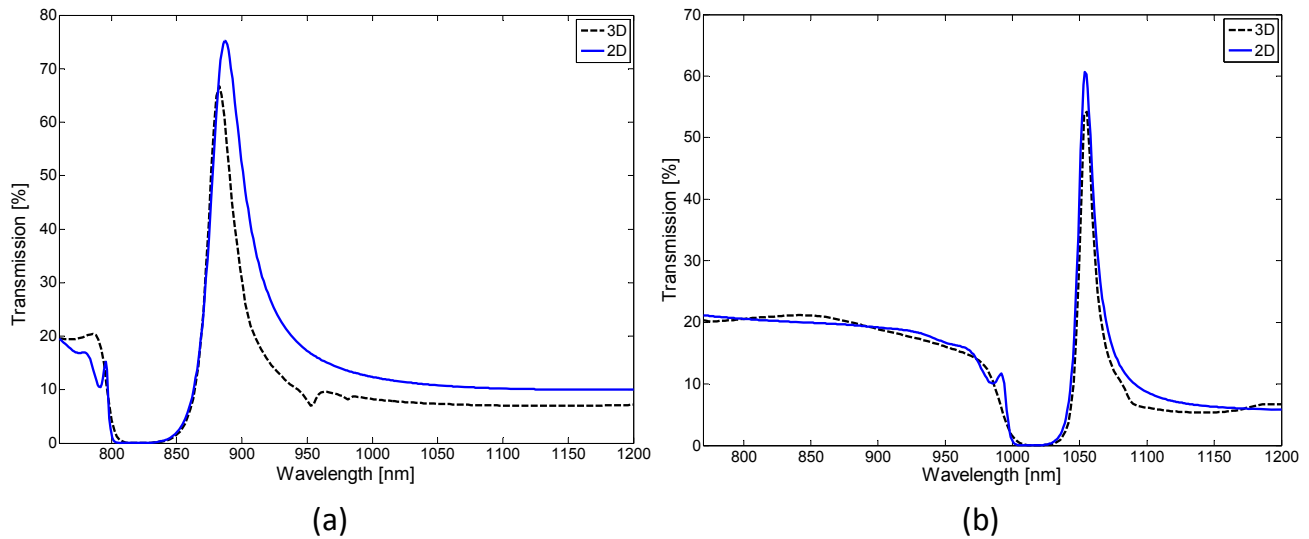


Fig.3. Comparison of the transmission spectra of a 1-D (blue solid line) and 2-D (black dashed line) periodic arrays with (a) $p = p_1 = p_2 = 800 \text{ nm}$ and (b) $p = p_1 = p_2 = 1000 \text{ nm}$.

Moreover, as Fig. 4 clearly demonstrates, relatively small variations, due to the spatial discretization of the computational domain, occur when the electric field is rotated in-plane: the plasmonic band gap and the zero-transmission state do not undergo any shift from $\theta = 0$ to $\theta = \pi/2$. This behavior can be explained by decoupling the incident electric field in two components along the directions of the periodicities. Since each component experiences the same periodicity ($p_1 = p_2$), their recombination does not alter the spectral response of the squared array of patches regardless of the angle θ . We can thus state that, in the hypotheses of normal incidence and equal dimensions ($p = p_1 = p_2$), transmission diagrams obtained considering a 1-D array of nanoslits illuminated by a TM-polarized input beam are exactly the same of those of a 2-D periodic arrays illuminated by a source field with any polarization.

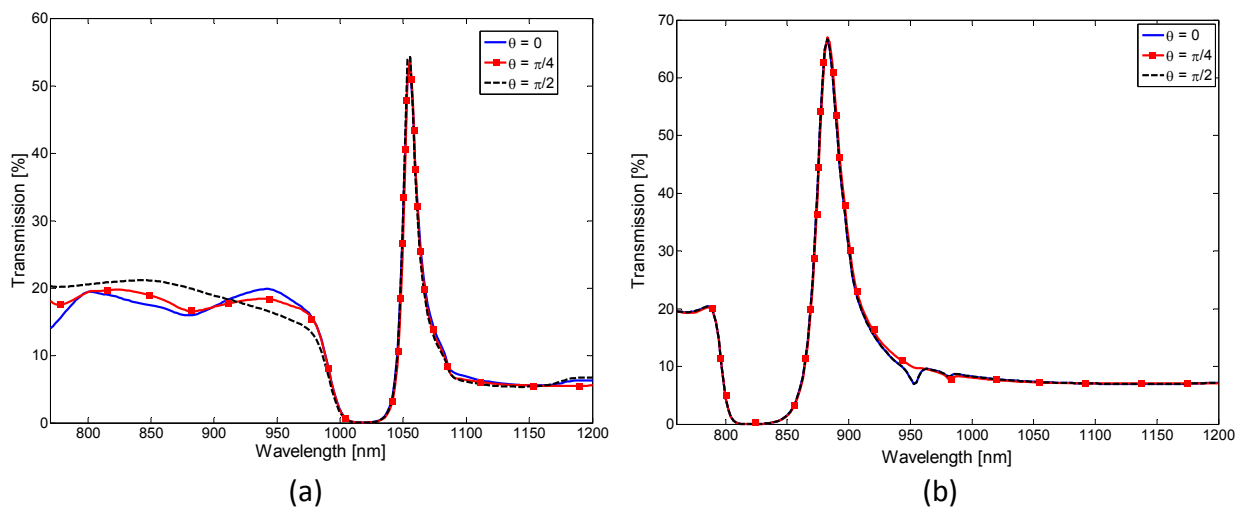


Fig.4. Comparison of transmission spectra of the 2-D periodic array for different angles θ for (a) $p = p_1 = p_2 = 800 \text{ nm}$ and (b) $p = p_1 = p_2 = 1000 \text{ nm}$.

More convincing evidence of the analogy of the structures in Fig.1(a) and (b) is provided by Figs.5 (a) and (b), where the magnetic field intensity of the zero transmission state is plotted for both arrays with 1-D (Fig.5(a)) and 2-D (Fig.5(b)) periodicities. In particular, Fig.5 plots the magnetic field intensity for $m_2 = 1010.7 \text{ nm}$ (see Fig.2), where the transmission is virtually zero and reflection values approach 98%¹⁶. It is worth noting that Fig.5(b) shows only one section of the magnetic field in the 3D structure, while the inset provides a complete view of the simulated cell. Results in Fig.5 show a magnetic field perfectly settled on each element of the array, thus providing the proof of the formation of a standing wave over the input surface of both arrays.

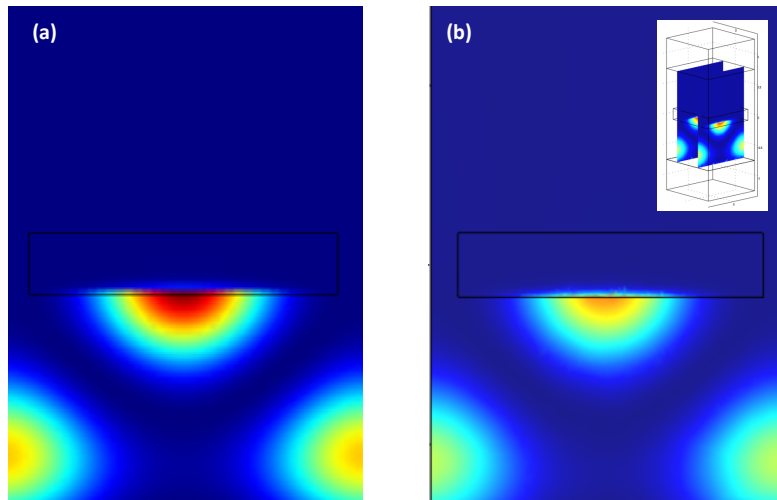


Fig.5. Magnetic field intensity of the zero-transmission state ($\lambda = 1010.7 \text{ nm}$) for arrays with 1-D (a) and 2-D (b) periodicities; Inset in (b): complete three-dimensional view of the array.

3. BAND GAP FORMATION AND TRANSITION IN 2-D RECTANGULAR ARRAY

In this section, the difference between 1-D and 2-D arrays will be highlighted through an accurate description of the dependence of transmission diagrams on the variation of the rotation angle θ . The simulations are performed on the structure in Fig.1(b) where $p_1 \neq p_2$. While the array of square patches does not exhibit changes in the spectral response regardless of θ , with excellent overlap of the transmission curves (see Figs. 4(b) and 5(b)), different periodicities can now alter dramatically the response of the system: the spectrum is modulated by the opening and closing of band gaps as a function of θ . Fig.6 in fact proves that the two periodicities are actually acting independently: the transmission diagram changes as a function of θ ranging from 0 to $\pi/2$, i.e. from the case with $p_1 = 800 \text{ nm}$ to that with $p_2 = 1000 \text{ nm}$. This analysis clearly demonstrates that the spectral response gradually changes between two different borderline cases, corresponding to the matching conditions between the unperturbed SPP wavelength and the two periodicities, p_1 and p_2 . Here, 1-D and 2-D periodic arrays do not show the same spectral response, since the 2-D one is strongly dependant on the polarization of the exciting field. Finally, this analysis also proves that physical and geometrical parameters can be optimized in order to engineer the spectral behavior of the actual structure, by broadening the gap extension or by modifying its spectral position

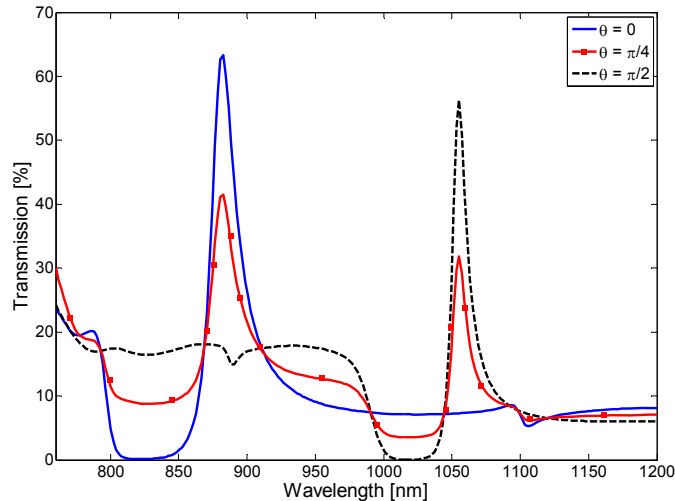


Fig.6. Transmission spectra of the 2-D periodic array having a rectangular shape ($p_1 = 800 \text{ nm}$, $p_2 = 1000 \text{ nm}$) for different angles θ .

4. CONCLUSIONS

In conclusion we have demonstrated that the spectral response of 2-D periodic arrays of gold patches exhibits forbidden bands whenever the effective wavelength of the unperturbed SPP of the air-metal or dielectric-metal interface matches the periodicity of the structure. All the features of 2-D periodic structures, i.e. plasmonic band gap and related resonances, are reproduced in 1-D systems. Position, extension and sharpness of such bands depend on the geometrical parameters of metal patches and on the optical properties of surrounding media. We have shown that squared arrays of gold patches are insensitive to the angle of incidence, whereas the transmission spectrum for rectangular arrays of gold patches is strongly dependent on the angle of the impinging field. We hope this study will serve to stimulate the search for many new plasmonic devices, where a specific polarization behavior is required, such as patterned metal reflectors for thin film solar cells to achieve reflectivity values as close as possible to 100 %. At the same time, these features can also lead to the development of new polarization sensitive optical filters, switches and sensors operating in a wide optical range spanning from visible to infrared frequencies.

REFERENCES

- [1] Ebbesen, T.W., Lezec, H.J., Ghaemi, H.F., Thio T., and Wolff, P. A. ,“Extraordinary Optical Transmission through Subwavelength Hole Arrays,” *Nature* 391, 667 (1998).
- [2] Garcia-Vidal, F.J., Lezec, H.J., Ebbesen, T.W. and Martin-Moreno, L., “Multiple Paths to Enhance Optical Transmission through a Single Subwavelength Slit,” *Phys. Rev. Lett.* 90, 213901 (2003).
- [3] Kihm, J.E., Yoon, Y.C. , Park, D.J. , Ahn, Y.H. , Ropers, C. , Lienau, C., Kim, J. , Park Q.H., and Kim, D.S. , “Fabry-Pérot Tuning of the Band-gap Polarity in Plasmonic Crystals,” *Phys. Rev. B* 75, 035414 (2007).
- [4] Vincenti, M.A., Petruzzelli, V., Prudenzano, F., D’Orazio, A., Bloemer, M.J., Akozbek, N. and Scalora, M., “Second harmonic generation from nanoslits in metal substrates: applications to palladium-based H₂ sensor,” *J. Nanophotonics* 2, 021851 (2008).
- [5] Vincenti, M.A., D’Orazio, A., Buncick, M., Akozbek, N., Bloemer, M.J. and Scalora, M., "Beam steering from resonant sub-wavelength slits filled with a nonlinear material," *J. Opt. Soc. B* 26, 301-307 (2009).
- [6] Marrocco, V., Grande, M., Marani, R., Calò, G., Petruzzelli, V., D’Orazio, A., Stomeo, T., De Vittorio, M., Passaseo, A., "Plasmonic nanostructure for enhanced light concentration devoted to photovoltaic applications," *Proceedings of International Conference on Transparent Optical Network, Mo.C2.3* (2010).
- [7] Xie, Y., Zakharian, A. R., Moloney, J. V. and Mansuripur, M., “Transmission of Light through a Periodic Array of Slits in a Thick Metallic Film,” *Opt. Express* 13, 4485 (2005).
- [8] Pacifici, D., Lezec, H. J., Atwater, H. A. and Weiner, J., “Quantitative Determination of Optical Transmission through Subwavelength Slit Arrays in Ag Films: Role of Surface Wave Interference and Local Coupling between Adjacent Slits,” *Phys. Rev. B* 77, 115411 (2008).
- [9] Vincenti, M.A., de Ceglia, D., Buncick, M., Akozbek, N., Bloemer, M.J. and Scalora, M., “Extraordinary Transmission in the Ultraviolet Range from Subwavelength Slits on Semiconductors,” *J. Appl. Phys.* 107, 053101 (2010).
- [10] Palik, E.D., [Handbook of Optical Constants of Solids], Academic Press, San Diego (1985).
- [11] COMSOL Multiphysics 3.5a, <http://www.comsol.com>.
- [12] Vincenti , M. A., De Sario, M., Petruzzelli, V., D’Orazio, A., Prudenzano, F., de Ceglia, D., Akozbek., N., Bloemer, M.J., Ashley, P. and Scalora, M., "Enhanced transmission and second harmonic generation from subwavelength slits on metal substrates," *Proceedings of SPIE* 6987, 69870O (2008).
- [13] Porto, J. A. , García-Vidal, F. J. and Pendry, J. B., “Transmission resonances on metallic gratings with very narrow slits,” *Phys. Rev. Lett.* 83, 2845 (1999).
- [14] Fernandez-Dominguez, A. I., García-Vidal, F. J. and Martín-Moreno, L., “Resonant transmission of light through finite arrays of slits,” *Phys. Rev. B* 76, 235430 (2007)
- [15] Moreno, E., Martín-Moreno, L. and García-Vidal, F. J., “Extraordinary optical transmission without plasmons: the s-polarization case,” *J. Opt. A* 8, S94–S97 (2006).
- [16] Marani, M., Grande, M., Marrocco, V., D’Orazio, A., Petruzzelli, V., Vincenti, M.A., de Ceglia, D., “Plasmonic Band Gap formation in two-dimensional periodic arrangements of gold patches with sub-wavelength gaps,” submitted to *Optics Letters* (2010).